Chapter 19
Pathways to Unification with Vector Like Fermions

Biplob Bhattacherjee, Ashwani Kushwaha, Pritibhajan Byakti, and Sudhir K. Vempati

Abstract We present a minimal extensions of Standard Model with TeV scale vector like fermions which leads to unification of gauge couplings. Model has been constraints from proton decay, Higgs stability and perturbativity. The simplest models contain copies of vector like fermions in two different (incomplete) representations. Some models enclose SU(2) triplet, Type III seesaw mechanism for neutrino masses whereas some others have a dark matter candidate. In all the models, at least one of the candidates has non-trivial representation under $SU(3)_{color}$. In the limit of vanishing Yukawa couplings, new QCD bound states are formed, which can be probed at LHC. The present limits based on results from 13 TeV already probe these particles for masses around a TeV.

19.1 Introduction

Grand Unification the one of the elegant solutions which could explain the hierarchy between the strong, weak and electromagnetic forces. The three separate gauge couplings unify in to a single one at some high scale $\sim 10^{(15-16)}$ GeV; a single gauge group like $SU(5)$ would suffice to explain all the three interactions at those scales. GUTs (Grand Unified theories) have been very popular due to various other features they predicted like proton decay, fermion mass relations including top-bottom yukawa unification, charge quantisation, weak mixing angle etc. It has been noticed

B. Bhattacherjee · A. Kushwaha · P. Byakti · S. K. Vempati (✉)
Centre for High Energy Physics, Indian Institute of Science, C. V. Raman Avenue, Bangalore 560012, India
e-mail: vempati@iisc.ac.in

A. Kushwaha
INFN-Sezione di Napoli, Complesso Universitario di Monte S. Angelo, Via Cintia Edificio 6, 80126 Napoli, Italy

P. Byakti
Department of Physics, Pandit Deendayal Upadhyaya Adarsha Mahavidyalaya (PDUAM) Eraligool, Karimganj 788723, Assam, India

A. Giri and R. Mohanta (eds.), *Workshop on Frontiers in High Energy Physics 2019*, Springer Proceedings in Physics 248,
https://doi.org/10.1007/978-981-15-6292-1_19

that Grand Unified theories have a hierarchy problem which manifests itself as large uncontrolled quantum corrections to the Standard Model Higgs boson mass of the order of GUT scale. Furthermore it has been noticed after the results from CERN's LEP-I, the Standard Model gauge couplings do not unify precisely at the GUT scale.

Supersymmetric Grand Unified theories on the other hand offer a resolution to these problems. They solve the hierarchy problem by cancelling the dangerous quadratic and large logarithmic corrections and furthermore lead to a precise unification of the Standard Model gauge coupling constants. The supersymmetric grand unification has been pursued in great detail over the last few decades and is still perhaps the most popular physics beyond standard model (BSM). It also ties naturally with String theory. While supersymmetric grand unification still remains the most attractive path, it is still important to keep an open eye for other possibilities especially given that LHC has so far not seen any signature of supersymmetric particles.

In the recent years, there have been other solutions for the hierarchy problem. Perhaps one of the most radical and remarkable of them is the relaxion solution [1] which uses a cosmological evolution of the Higgs particle in a potential generated by an axion like field, leading it to be trapped at a particular point. While this is indeed an interesting idea, it leads to no new physics around the weak scale. In this kind of scenarios, there will be a desert at least up to 10^6 GeV and further beyond. Depending on the variations of the mechanism, there need not be no new physics to solve the hierarchy problem all the way up to the GUT scale.

We are interested in the extensions of the Standard Model with this kind of the solutions to the hierarchy problem in mind. The question we asked is how to realise Grand Unification in this set up. Gauge coupling unification will not be possible unless there is some extension of the Standard Model matter spectrum. We consider vector-like fermions which lead to precision gauge coupling unification (for earlier works in this direction, please see [2–16]). There are other features of these models which makes them appealing. The constraints from electroweak precision parameters remain small, especially from S and T parameters [17, 18], as long as the mixing between vector-like fermions and SM fermions is small. There are no gauge anomalies as they are vector in nature. And further, they can be tested directly at the collider experiments like LHC. In these models as we will see the Higgs potential naturally remains stable all the up to the GUT scale. In the view that the primary existence of these vector particles is unification of gauge couplings, we dub them "unificons" [19]. However, as we will see later, these models do not restrict themselves only to unification. In some models, we find solutions with a provision for Type III seesaw mechanism for neutrino masses, and in some others there is a dark matter candidate. Thus "unificon" models can indeed have wide phenomenological reach solving other problems in Standard Model like neutrino masses and dark matter.

As a search for all possible models with extra vector-like fermions would be a herculean task, we resort to minimality. We assume unification of gauge couplings á la SU(5). Additional vector-like particles appear as incomplete representations of SU(5). We have looked at all possible incomplete decompositions emanating from SU(5) representations up to dimension 75. The number of copies in each representation is taken to be n which is an integer between 1 and 10. The mass range of these

additional vector-like fermions is chosen to be $m \sim k$ TeV, where k is a $\mathcal{O}(1)$ number taken to be approximately between 1/4–5.

19.2 Renormalization Group Equation

19.2.1 One Loop Gauge Unification

The gauge couplings do not unify precisely in the Standard Model. If one insists on unification of the guage couplings at the GUT scale, the required $\sin^2\theta_W(M_Z^2)$ is 0.204 (for one loop beta functions) instead of the current experimental value of $\sin^2\theta_W(M_Z^2) = 0.23129 \pm 0.00005$ [20]. We look for additional vector-like matter fermions, close to the weak scale, which can compensate the deviation and lead to successful gauge coupling unification. At the 1-loop level, the beta functions for the three gauge couplings are given as

$$\frac{dg_l}{dt} = -\frac{1}{16\pi^2} b_l g_l^3, \text{ where } t = \ln\mu, \tag{19.1}$$

where is $l = \{U(1), SU(2), SU(3)\}$ runs over all the three gauge groups. The b_l functions have the general form:

$$b_l = \Big[\frac{11}{3}C(V_l) - \frac{2}{3}T(F_l) - \frac{1}{3}T(S_l)\Big]. \tag{19.2}$$

Here $C(R)$ is quadratic Casimir and $T(R)$ is Dynkin index of representation R. V, F and S represents vector, Weyl fermion and complex scalar field respectively. For U(1) group $T(R_1)$ and $C(R_1)$ are

$$T(R_1) = C(R_1) = \frac{3}{5}Y^2. \tag{19.3}$$

In the presence of a vector-like fermion V_1 at the scale M_1 greater than weak scale, given the gauge coupling unification at M_{GUT}, the (19.1) take the form:

$$\alpha_l^{-1}(\mu_{in}) = \frac{b_l^0}{2\pi}\ln\frac{\mu_{in}}{M_{GUT}} + \frac{b_l^{V_1}}{2\pi}\ln\frac{M_1}{M_{GUT}} + \alpha_l^{-1}(M_{GUT}), \tag{19.4}$$

where $\alpha_l = \dfrac{g_l^2}{4\pi}$ and $b_l^{V_1}$ capture effect of addition of vector-like fermions at the scale M_1. The parameter $\bar{b}$ is an useful measure of unification of gauge couplings. It is defined as

$$\bar{b}(\mu_{in}) = \frac{\alpha_3^{-1}(\mu_{in}) - \alpha_2^{-1}(\mu_{in})}{\alpha_2^{-1}(\mu_{in}) - \alpha_1^{-1}(\mu_{in})} \tag{19.5}$$

$$= \frac{\triangle b_{32}^0 + \left(\triangle b_{32}^{V_1}\right) \ln(M_1/M_{GUT})/\ln(\mu_{in}/M_{GUT})}{\triangle b_{21}^0 + \left(\triangle b_{21}^{V_1}\right) \ln(M_1/M_{GUT})/\ln(\mu_{in}/M_{GUT})}. \tag{19.6}$$

where the second line can be derived from (19.4) assuming unification at M_{GUT}. The parameters Δb_{lk} are defined as $b_l - b_k$. In the absence of new vector-like particles, $\bar{b}$ is independent of the running scale μ. In their presence however, there is a μ dependence but it is typically mild. For the case where the new particles are close to weak scale $\sim$ TeV, and when $\mu_{in} = M_Z$, the log factor, $\ln(M_1/M_{GUT})/\ln(\mu/M_{GUT})$ is close to one. In this case, the expression for unified theories is given by

$$\bar{b} = \frac{\triangle b_{32}^0 + \triangle b_{32}^{V_1}}{\triangle b_{21}^0 + \triangle b_{21}^{V_1}} \tag{19.7}$$

Note that the (19.5) can purely be determined from experiments at M_Z. Its value is given by

$$\bar{b}(M_Z) = 0.718, \tag{19.8}$$

In the SM, if we insist on unified gauge couplings at M_{GUT}, at the weak scale, $\bar{b}$ takes the value 0.5 clearly in conflict with experiments. In MSSM, $\bar{b}$ turns out to be 5/7. Of course, these arguments are valid only at one loop. There is deviation in (19.7) when higher loops are considered.

19.2.2 Two Loop RG Evolution of Gauge Couplings

To improve the precision in unification of gauge couplings, we consider two loop beta functions. At the two loop level, the beta functions involve Yukawa couplings which makes them model dependent. In the present analysis, we restrict ourselves to models with minimal or zero vector-like fermion and SM mixing through the Higgs mechanism. With this assumption, we can safely neglect the Yukawa contribution from the new sector to the gauge coupling unification. The RG equations at the two loop level are given by [21, 22]:

$$\frac{dg_l}{dt} = -b_l \frac{g_l^3}{16\pi^2} - \sum_k m_{lk} \frac{g_l^3 g_k^2}{(16\pi^2)^2} - \frac{g_l^3}{(16\pi^2)^2} Tr\left\{C_{lu} Y_u^\dagger Y_u + C_{ld} Y_d^\dagger Y_d + C_{le} Y_e^\dagger Y_e\right\}, \tag{19.9}$$

where the first term in the right hand side is due to one-loop which was discussed in the previous subsection. The second term is purely from gauge interactions whereas

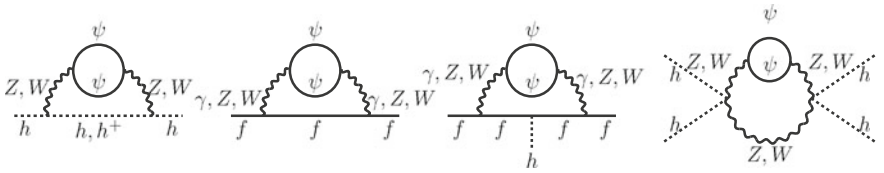

Fig. 19.1 Diagrams contributing in two loop RG of Yukawa and Higgs quartic couplings, through new Fermion fields (ψ). Here f is any standard model fermion. First two diagrams correspond to anomalous dimension and the last two diagrams are giving vertex corrections

the third terms involves the Yukawa terms $Y_{u,d,e}$ where the suffixes mean the up-type, down-type and lepton-type couplings. The expression for the coefficients appearing in the second term of the above equation are as follows [21]:

$$m_{lk} = \left(2C(F_k)d(F_k)T(F_l)d(F_m) + 4C(S_k)d(S_k)T(S_k)d(S_m)\right) \text{ where } l \neq k \tag{19.10}$$

$$m_{ll} = \left[\frac{10}{3}C(V_l) + 2C(F_l)\right]T(F_l)d(F_m)d(F_k) + \left[\frac{2}{3}C(V_l) + 4C(S_l)\right]T(S_l)d(S_m)d(S_k) - \frac{34}{3}[C(V_l)^2], \tag{19.11}$$

where $d(R)$ means dimension of the representation R and other factors C(R) and T(R) are already defined in (19.2).

As we are considering the Yukawa couplings between the vector-like fermions with Higgs boson to be negligible,[1] the contribution of vector-like particles to C_{lf} coefficient can be taken as zero. On the other hand $\delta m_{ij} \neq 0$, where δ is used to indicate contribution from additional vector-like fermions. The explicit values of δm_{ij} for each of the viable models can be found in [19].

Two-loop RG running for the Yukawa couplings is given as

$$Y_{u,d,e}^{-1}\frac{dY_{u,d,e}}{dt} = \frac{1}{16\pi^2}\beta_{u,d,e}^{(1)SM} + \frac{1}{(16\pi^2)^2}\beta_{u,d,e}^{(2)SM} \tag{19.12}$$

The SM RG for these Yukawa couplings are shown in [19]. Two loop beta functions get contributions from the diagrams shown in Fig. 19.1, which results in the following terms:

$$\begin{aligned}
\delta\beta_u^{(2)V} &= \frac{40}{9}g_3^4T(F_3)d(F_2)d(F_1) + \frac{29}{90}g_1^4T(F_1)d(F_3)d(F_2) + \frac{1}{2}g_2^4T(F_2)d(F_3)d(F_1)\\
\delta\beta_d^{(2)V} &= \frac{40}{9}g_3^4T(F_3)d(F_2)d(F_1) - \frac{1}{90}g_1^4T(F_1)d(F_3)d(F_2) + \frac{1}{2}g_2^4T(F_2)d(F_3)d(F_1)\\
\delta\beta_e^{(2)V} &= \frac{11}{10}g_1^4T(F_1)d(F_3)d(F_2) + \frac{1}{2}g_2^4T(F_2)d(F_3)d(F_1)
\end{aligned} \tag{19.13}$$

[1] This can be organised by imposing discrete symmetries distinguishing SM partners from vector-like fermions.

Higgs Self Coupling The modification of the gauge beta functions in the presence of additional vector-like particles can have implications on the evolution of the Higgs self coupling. The evolution of the SM Yukawa couplings is itself modified in these models. We followed [23], beta function of the λ at the two loop and put a condition that λ is always positive at all scales of evolution. Two-loop RG running for the Higgs quartic coupling are

$$\frac{d\lambda}{dt} = \frac{1}{16\pi^2}\beta_\lambda^{(1)SM} + \frac{1}{(16\pi^2)^2}\beta_\lambda^{(2)SM}, \tag{19.14}$$

where beta functions for SM Higgs quartic couplings are defined in [19]. The effect of new fermion fields in RG of Higgs quartic couplings are:

$$\begin{aligned}\delta\beta_\lambda^{(2)V} = &-\frac{1}{25}g_1^4\left(12g_1^2 + 20g_2^2 - 25\lambda\right)T(F_1)d(F_3)d(F_2)\\ &-\frac{1}{5}g_2^4\left(4g_1^2 + 20g_2^2 - 25\lambda\right)T(F_2)d(F_3)d(F_1)\end{aligned} \tag{19.15}$$

To solve the RG equations we need boundary values of the coupling constants and masses at the top mass (M_t) scale. The quantities of interest are Higgs quartic coupling (λ), Yukawa couplings and gauge coupling, which can be calculated in terms of physical observables W-boson mass (M_W), Z-boson mass (M_Z), Higgs mass (M_h) and $\alpha_3(M_Z)$ at the two loop level. The input parameters are calculated in the $\overline{MS}$-scheme. More detailed can be found in [19, 23].

Proton Decay For these models, using the simple decay width formulae, $\Gamma \sim \alpha_{Gut}\frac{m_{proton}^5}{M_{GUT}^4}$ we estimate the life time of the proton, where the current experimental value is of order $> 10^{32} - 10^{34}$ years [24].

Threshold Corrections at GUT Scale To study the impact of threshold corrections on gauge coupling unification, we define the following parameters: $\alpha_{ave.}(\mu) = (\alpha_1(\mu) + \alpha_2(\mu) + \alpha_3(\mu))/3$ and $\bar{\Delta}_i(\mu) = (\alpha_i(\mu) - \alpha_{avg}(\mu))/\alpha_{ave}(\mu)$. Note that α_{ave} coincides with α_{GUT} when all $\bar{\Delta}_i \to 0$, at the scale M_{GUT}. In the presence of threshold corrections, one could allow for deviations in α_{GUT} in terms of $\bar{\Delta}_i$ at the GUT scale. Defining $\Delta = max(\bar{\Delta}_i)$, we see that Δ is as large as 6% in the Standard Model. In our survey of models below, we have allowed for variations in Δ up to 1.2%.

19.3 Gauge Coupling Unification with Vector-Like Fermions

In our search, we focus on vector-like matter in incomplete representations of SU(5). We have considered (incomplete) representations [25] up-to dimension 75. The full list of incomplete representations is presented in Appendix A. As can be seen from

the Table 19.2, there are 40 representations which we have considered. We found no successful models for $i = 1$ even with $n_1 = 6$. The simplest solutions we found contain at least two different representation content each with a different number of copies. We call these solutions "minimal unificon models". These are listed in Table 19.1. The two representations considered are called Rep.1 and Rep2. The representation is described as $n_i(R_{SU(3)}, R_{SU(2)}, R_{U(1)})$, where n_i introduced earlier is the number of copies of the representation, R_G is the representation of the field under the gauge group G of the SM.

Furthermore, in the above, we mentioned only one part of the representation instead of the complete vector multiplet for brevity. The second last column, entries are written in units of 10^{16} GeV. All models appeared as the solution of one loop RG equation. Third and fifth columns show's the mass range of the vector-like fields.

The list of such of models is given in Table 19.1. Several interesting features are evident. The minimalist model is model 7, with only two vector-like fermions. These model are constraints from direct searches of vector-like quarks at LHC and elsewhere if there is significant mixing with SM particles. In its absence, as we assumed here, the bound will be different. We would discuss one of the model in detail.

19.3.1 Model 2

We got six copies of Rep1 $= \left(1, 2, \frac{1}{2}\right)$ in mass range between 250–2000 GeV and two copies of Rep2 $= (8, 1, 0)$ with mass range from 500 GeV to 5 TeV. Rep1 field is lepton doublet like field, lightest neutral component of these fermions can be a dark matter candidate. Rep2 is gluino like and at the renormalisation level, it can interact with the gluons only and does not have any decay chain.

In the model, M_{Rep1} is always less than M_{Rep2}. A sample unification point is shown in Fig. 19.2a, six copies of lepton like vector fermions with degenerate mass of 620 GeV and two copy of Rep2 with a mass of 4310 GeV is considered. The figure shows unification of gauge couplings as well as running of y_t and λ. Mass distribution in Rep1-Rep2 mass plane is shown in Fig. 19.2b.

19.4 Collider Signature of Minimal Vector-Like Fermion Models

In this section we will show the pair-produced colored particles from BSM senarios can be constrained through the non- observation of dijet and other resonances arising from their QCD bound states. In the following we will concentrate on the strongly interacting exotic sector; which appears in all the successful models.

Table 19.1 Model with two vector-like fermions representation satisfying gauge coupling unification and vacuum stability condition, considering $\triangle$ of 1.2%

Mod No.	Rep 1	M_{Rep1} GeV	Rep 2	M_{Rep2} GeV	One loop	Two loop	Vaccum stability	$M_{\text{GUT}} \times 10^{16}$ GeV	α_{GUT}
1	$6\left(1, 2, \frac{1}{2}\right)$	$(250 - 5000)$	$1\left(6, 1, \frac{1}{3}\right)$	$(250 - 5000)$	✓	✓	✓	∼0.11	∼0.038
2	$6\left(1, 2, \frac{1}{2}\right)$	$(250 - 2000)$	$2\ (8, 1, 0)$	$(500 - 5000)$	✓	✓	✓	∼2.34	∼0.040
3	$2\ (1, 3, 0)$	$(250 - 5000)$	$4\left(3, 1, \frac{1}{3}\right)$	$(250 - 5000)$	✓	✓	✓	∼2.29	∼0.030
4	$2\left(3, 1, \frac{2}{3}\right)$	$(250 - 5000)$	$2\left(3, 2, \frac{1}{6}\right)$	$(250 - 4500)$	✓	✓	✓	∼ 4.79	∼0.040
5	$3\ (1, 3, 0)$	$(1800 - 5000)$	$1\left(6, 1, \frac{2}{3}\right)$	$(250 - 950)$	✓	✓	✓	∼1.08	∼0.037
6	$1\left(1, 4, \frac{1}{2}\right)$	$(250 - 2000)$	$2\left(6, 1, \frac{2}{3}\right)$	$(1000 - 5000)$	✓	✓	✓	∼8.58	∼0.107
7	$1\left(3, 1, \frac{1}{3}\right)$	$(250 - 5000)$	$1\left(3, 2, \frac{1}{6}\right)$	$(250 - 5000)$	✓	✓	✓	∼2.20	∼0.028
8	$4\left(1, 2, \frac{1}{2}\right)$	$(300 - 5000)$	$1\ (8, 1, 0)$	$(300 - 5000)$	✓	✓	✓	∼0.10	∼0.030
9	$3\ (1, 3, 0)$	$(1100 - 5000)$	$6\left(3, 1, \frac{1}{3}\right)$	$(250 - 1800)$	✓	✓	✓	∼25.0	∼0.037

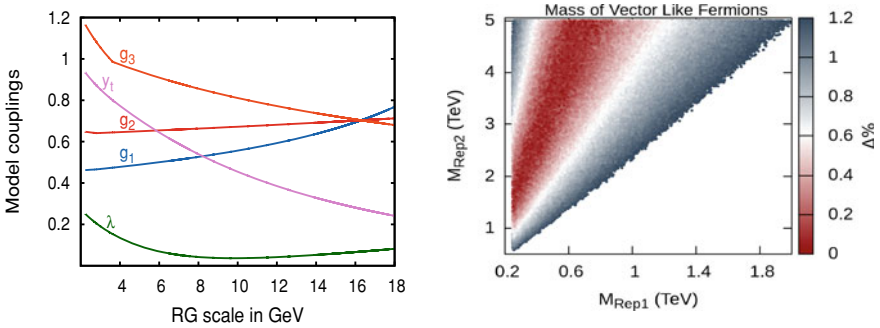

(a) (b)

Fig. 19.2 Model 2: Fig. **a** Gauge couplings (g_1,g_2,g_3) unification and vacuum stability ($\lambda > 0$) plot, considering vector-like fermion in Rep1 of mass 620 GeV and Rep2 of mass 4310 GeV. Figure **b** Mass range allowed for vector-like fermions in Rep1 and Rep2 for gauge unification and vacuum stability

19.4.1 Formalism for Bound State

We investigate the possibility of producing bound states of the colour vector-like fermions. For the formation of bound state, we assume the new vector-like fermion (ψ) is long lived. The bound state formalism has been studied in [26, 27], where they focus on pair-produced colour particle Beyond the Standard Model by the observation of diphoton, dijet etc. resonances arising from QCD bound state.

A pair of $\psi\bar{\psi}$ near threshold can form a QCD bound state, which we defined as $\mathcal{O}$. For particles (ψ) of mass $m_\psi \gg \Lambda_{QCD}$, we can estimate bound state as modified hydrogenic approximation. For a particle ψ in the colour representation R, the potential between ψ and $\bar{\psi}$ depends on the colour representation $\mathcal{R}$ of the $\psi\bar{\psi}$ pair through the casimirs of R and $\mathcal{R}$ as

$$V(r) = -C\frac{\bar{\alpha}_s}{r}, \qquad C = C(R) - \frac{1}{2}C(\mathcal{R}) \tag{19.16}$$

where $\bar{\alpha}_s$ is defined as the running coupling at the scale of the average distance between the two particle in the corresponding hydrogenic state, which is order of the Bohr radius $a_0 = 2/(C\bar{\alpha}_s m_\psi)$. The production cross-section of any narrow resonance $\mathcal{O}$ of mass M and spin J from parton x and y, and the decay rate of bound state to x and y, are related by

$$\hat{\sigma}_{xy\to\mathcal{O}} = \frac{2\pi(2J+1)d_{\mathcal{O}}(\mathcal{R})}{D_x D_y}\frac{\Gamma_{\mathcal{O}\to xy}}{M}2\pi\delta(\hat{s} - M^2) \qquad (\times 2 \text{ for x = y}) \tag{19.17}$$

where $D_{\mathcal{O}}$ denotes the colour representation of particle $\mathcal{O}$.

In the next subsection we will strict ourself to study the colour singlet and spin zero ($J = 0$) bound state system. Assuming the production cross-section of $\psi\bar{\psi}$ is dominated by gluon fusion. The gluon fusion partonic production cross-section of of bound state is given by

$$\hat{\sigma}_{gg\to\mathcal{O}} = \frac{\pi^2}{8}\frac{\Gamma_{\mathcal{O}\to gg}}{M}\delta(\hat{s} - M^2) \tag{19.18}$$

Depending on the quantum number of ψ, bound state $\mathcal{O}$ can decay to diphoton, dijet, $Z\gamma$, ZZ and W^+W^- channels. The production of preceding pair events produced in proton-proton collisions in LHC can be predicted as $\sigma(pp \to \mathcal{O}) \times BR(\mathcal{O} \to X_1X_2)$.

19.4.2 Signals $\gamma\gamma$ and Dijet Chennel

Any spin half particle can be produced in pairs (in gg collisions) in an S-wave $J = 0$ colour singlet bound state, which can decay as typically narrow $\gamma\gamma$, ZZ, $Z\gamma$ and gg resonance. There has been searches in $Z\gamma$, ZZ and WW resonances from these bound states. They all remain less sensitive than $\gamma\gamma$ channel. Hence, we show here the channel $\gamma\gamma$. The decay width of the $\gamma\gamma$ signal due to spin $J = 0$ bound state is given as:

$$\Gamma(\mathcal{O}^{\mathcal{R}}_{J=0} \to \gamma\gamma) = \frac{Q^4 C(R)^3 d_R}{2}\alpha^2\bar{\alpha}_s^3 m_\psi \tag{19.19}$$

S-wave bound state with spin $J = 0$ can be produced via $gg \to \mathcal{O}$ and annihilating mostly to gg. For $j = 1/2$ there is also a comparable contribution from S-wave $J = 1$ colour octet bound states produced via $q\bar{q} \to \mathcal{O}$ and annihilating to $q\bar{q}$, which we will not discuss here.

The decay width of gg signal due to spin $J = 0$ colour singlet bound state is,

$$\Gamma(\mathcal{O}^{\mathcal{R}=1}_{J=0} \to gg) = \frac{C(R)^5 d_R}{32}\alpha_s^2\bar{\alpha}_s^3 m_\psi \tag{19.20}$$

($\times 2$ for Complex Representation of constituent fermion)

19.4.3 Limits on Signals from CMS and ATLAS

In next section we examine the constraints on masses of bound state from dijet and diphoton bounds considering one copy of constituent vector-like fermions. We have used the recent limits of ATLAS and CMS for diphoton resonance at centre of energy

$\sqrt{s} = 13$ TeV from 2015 and as well as 2016 data. Dijet bounds has been considered for centre of energy $\sqrt{s} = 8$ and 13 TeV from both ATLAS and CMS.

19.4.3.1 Dijet Bounds

In Fig. 19.3a, b we present the $\sigma(pp \to \mathcal{O}) \times BR(\mathcal{O} \to gg)$ as a function of the mass of the $\mathcal{O}$ resonance considering one copy of constituent vector-like fermions. The black line is the upper limit on this cross-section from ATLAS [28] 8 TeV and blue line is from CMS [29] 8 TeV data in Fig. 19.3a. Figure 19.3b shows the dijet limits from ATLAS(black) [30] 13 TeV and CMS(blue) [31] 13 TeV data. We can clearly say that the dijet limits are not strong enough to rule any of the models, if they have only one copy of constituent fermions.

19.4.3.2 Diphoton Bounds

We present the production of diphoton channel as a function of the resonance mass considering one copy of constituent vector-like fermions in Fig. 19.4. Black line is the upper limit on this cross-section from ATLAS [32] 13 TeV and blue line is from CMS [33] 13 TeV data. It can be observed that the upper limits on cross-section can give stringent bound on the masses of vector-like fermions ($m_\psi = M/2$).

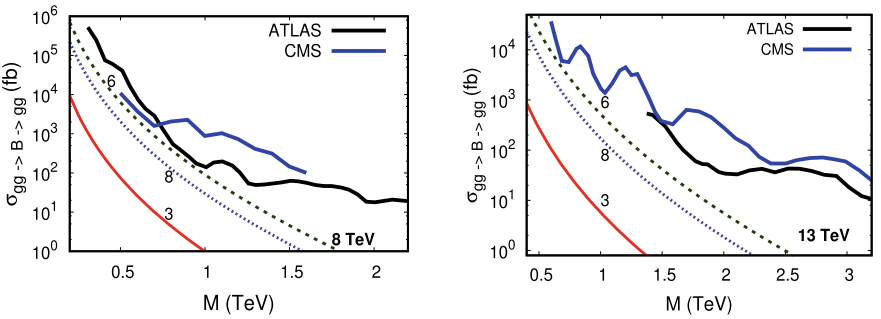

Fig. 19.3 Cross section of Dijet events at $\sqrt{s} = 8$ TeV (left) and $\sqrt{s} = 13$ TeV (right) for bound state of representation $\mathcal{R} = 1$ and $J = 0$, from constituent particle of representation $R = 3, 6, 8$. Limits from ATLAS 8 and 13 TeV are shown in thick black and CMS 8 and 13 TeV are shown in thick blue

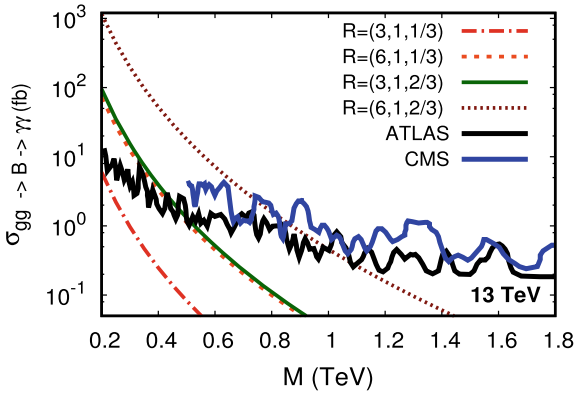

Fig. 19.4 Cross section of diphoton event w.r.t bound state mass at $\sqrt{s} = 13$ TeV for bound state of representation $\mathcal{R} = 1$ and $J = 0$ from constituent particle of color representation $R = 3, 6$. The red line(dash dot) shows the fermion with $R = 3$ and $Q = 1/3$, green line(solid) correspond to $R = 3$ and $Q = 2/3$, purple line(dotted) shows the fermion with $R = 6$ and $Q = 2/3$ and orange line(dashed) shows the $R = 6$ and $Q = 1/3$ fermion. Limits are from ATLAS 13 TeV black line and CMS 13 TeV blue line

19.5 Summary and Outlook

Grand Unified theories seems one of the most promising physics, beyond SM. We look for models with extra vector-like fermions at the weak scale which can lead to successful unification of gauge couplings. With two representation, we find a class of nine models leading to successful unification of gauge couplings. The coloured set of the vector-like fermions can be probed at LHC by looking for bound states formed by them and their probable decays. We have listed the present bounds from LHC for each successful model. Recently another work [34] has followed a similar direction and our results are consistent with each other.

Acknowledgements S. K. Vempati thanks the organisers of the conference FHEP-2019, at Hyderabad, India for a wonderful atmosphere. This work is supported by the CNRS LIA (Laboratoire International Associé) THEP (Theoretical High Energy Physics) and the INFRE-HEPNET (IndoFrench Network on High Energy Physics) of CEFIPRA/IFCPAR (Indo-French Centre for the Promotion of Advanced Research). SKV and AK are supported also CEFIPRA project "Glimpses of New physics" and Department of Science and Technology, Govt of India, Project "Nature of New Physics".

Appendix: Representations and Dynkin Indices

We considered all the $SU(3) \times SU(2) \times U(1)$ representations coming from $SU(5)$ representations upto dimension 75. In Table 19.2, we listed those forty representations

Table 19.2 Representation of fields considered in this paper. In the column entitled with "SM Rep" we put incomplete multiplets of $SU(5)$ and the entries inside the brackets are $SU(3)$, $SU(2)$ and $U(1)$ representations respectively. In the column with title we'd written the $SU(5)$ representations from which those representations are coming. Dynkin indices are calculated assuming the fields are scalar fields. Note that we had considered up the SU(5) representation of dimension 75. There are some extra representations as well

S.No.	SM Rep	Source	Dynkin indices	S.No.	SM Rep	Source	Dynkin indices
1	$(1, 1, 1)$	10	$\left(0, 0, -\frac{1}{5}\right)$	21	$\left(3, 2, \frac{7}{6}\right)$	$\overline{45}, \overline{50}$	$\left(-\frac{1}{3}, -\frac{1}{2}, -\frac{49}{30}\right)$
2	$(1, 1, 2)$	$\overline{50}$	$\left(0, 0, -\frac{4}{5}\right)$	22	$\left(3, 3, -\frac{1}{3}\right)$	45, 70	$\left(-\frac{1}{2}, -2, -\frac{1}{5}\right)$
3	$(1, 1, 3)$		$\left(0, 0, -\frac{9}{5}\right)$	23	$\left(3, 3, \frac{2}{3}\right)$	$\overline{35}, \overline{40}$	$\left(-\frac{1}{2}, -2, -\frac{4}{5}\right)$
4	$(1, 1, 4)$		$\left(0, 0, -\frac{16}{5}\right)$	24	$\left(\bar{3}, 3, \frac{4}{3}\right)$	70	$\left(-\frac{1}{2}, -2, -\frac{16}{5}\right)$
5	$(1, 1, 5)$		$(0, 0, -5)$	25	$\left(3, 4, \frac{7}{6}\right)$	$\overline{70'}$	$\left(-\frac{2}{3}, -5, -\frac{49}{15}\right)$
6	$\left(1, 2, \frac{1}{2}\right)$	5, 45, 70	$\left(0, -\frac{1}{6}, -\frac{1}{10}\right)$	26	$\left(6, 1, \frac{1}{3}\right)$	$\overline{45}$	$\left(-\frac{5}{6}, 0, -\frac{2}{15}\right)$
7	$\left(1, 2, -\frac{3}{2}\right)$	40	$\left(0, -\frac{1}{6}, -\frac{9}{10}\right)$	27	$\left(6, 1, -\frac{2}{3}\right)$	15	$\left(-\frac{5}{6}, 0, -\frac{8}{15}\right)$
8	$(1, 3, 0)$	24	$\left(0, -\frac{2}{3}, 0\right)$	28	$\left(6, 1, \frac{4}{3}\right)$	50	$\left(-\frac{5}{6}, 0, -\frac{32}{15}\right)$
9	$(1, 3, 1)$	15	$\left(0, -\frac{2}{3}, -\frac{3}{5}\right)$	29	$\left(\bar{6}, 2, \frac{1}{6}\right)$	35, 40	$\left(-\frac{5}{3}, -1, -\frac{1}{15}\right)$
10	$\left(1, 4, \frac{1}{2}\right)$	70	$\left(0, -\frac{5}{3}, -\frac{1}{5}\right)$	30	$\left(6, 2, \frac{5}{6}\right)$	75	$\left(-\frac{5}{3}, -1, -\frac{5}{3}\right)$
11	$\left(1, 4, -\frac{3}{2}\right)$	35	$\left(0, -\frac{5}{3}, -\frac{9}{5}\right)$	31	$\left(6, 2, -\frac{7}{6}\right)$	70	$\left(-\frac{5}{3}, -1, -\frac{49}{15}\right)$
12	$(1, 5, -2)$	$70'$	$\left(0, -\frac{10}{3}, -4\right)$	32	$\left(6, 3, \frac{1}{3}\right)$	$\overline{50}, \overline{70'}$	$\left(-\frac{5}{2}, -4, -\frac{2}{5}\right)$
13	$(1, 5, 1)$		$\left(0, -\frac{10}{3}, -1\right)$	33	$(8, 1, 0)$	24	$(-1, 0, 0)$
14	$(1, 5, 0)$		$\left(0, -\frac{10}{3}, 0\right)$	34	$(8, 1, 1)$	40	$\left(-1, 0, -\frac{8}{5}\right)$
15	$\left(3, 1, -\frac{1}{3}\right)$	5, 45, 50, 70	$\left(-\frac{1}{6}, 0, -\frac{1}{15}\right)$	35	$\left(8, 2, \frac{1}{2}\right)$	45, 50, 70	$\left(-2, -\frac{4}{3}, -\frac{4}{5}\right)$
16	$\left(\bar{3}, 1, -\frac{2}{3}\right)$	10, 40	$\left(-\frac{1}{6}, 0, -\frac{4}{15}\right)$	36	$(8, 3, 0)$	75	$\left(-3, -\frac{16}{3}, 0\right)$

(continued)

Table 19.2 (continued)

S. No.	SM Rep	Source	Dynkin indices	S. No.	SM Rep	Source	Dynkin indices
17	$\left(\bar{3}, 1, \frac{4}{3}\right)$	45	$\left(-\frac{1}{6}, 0, -\frac{16}{15}\right)$	37	$\left(\overline{10}, 1, 1\right)$	35	$\left(-\frac{5}{2}, 0, -2\right)$
18	$\left(3, 1, \frac{5}{3}\right)$	75	$\left(-\frac{1}{6}, 0, -\frac{5}{3}\right)$	38	$\left(\overline{10}, 2, \frac{1}{2}\right)$	$70'$	$\left(-5, -\frac{5}{3}, -1\right)$
19	$\left(3, 2, \frac{1}{6}\right)$	10, 15, 40	$\left(-\frac{1}{3}, -\frac{1}{2}, -\frac{1}{30}\right)$	39	$\left(15, 1, -\frac{1}{3}\right)$	70	$\left(-\frac{10}{3}, 0, -\frac{1}{3}\right)$
20	$\left(3, 2, -\frac{5}{6}\right)$	24, 75	$\left(-\frac{1}{3}, -\frac{1}{2}, -\frac{5}{6}\right)$	40	$\left(15, 1, \frac{4}{3}\right)$	$70'$	$\left(-\frac{10}{3}, 0, -\frac{16}{3}\right)$

[25] with their contribution to beta function (i.e. Dynkin index) considering them as scalar fields.

References

1. P.W. Graham, D.E. Kaplan, S. Rajendran, Cosmological relaxation of the electroweak scale. Phys. Rev. Lett. **115**(22), 221801 (2015)
2. C. Liu, Z.-H. Zhao, θ_{13} and the Higgs mass from high scale supersymmetry. Commun. Theor. Phys. **59**, 467–471 (2013)
3. T.G. Rizzo, Desert guts and new light degrees of freedom. Phys. Rev. D **45**, 3903–3905 (1992)
4. D.E. Morrissey, C.E.M. Wagner, Beautiful mirrors, unification of couplings and collider phenomenology. Phys. Rev. D **69**, 053001 (2004)
5. V. Barger, J. Jiang, P. Langacker, T. Li, String scale gauge coupling unification with vector-like exotics and non-canonical U(1)(Y) normalization. Int. J. Mod. Phys. A **22**, 6203–6218 (2007)
6. L. Calibbi, L. Ferretti, A. Romanino, R. Ziegler, Gauge coupling unification, the GUT scale, and magic fields. Phys. Lett. B **672**, 152–157 (2009)
7. I. Donkin, A. Hebecker, Precision gauge unification from extra Yukawa couplings. JHEP **09**, 044 (2010)
8. L.J. Hall, Y. Nomura, A finely-predicted higgs boson mass from a finely-tuned weak scale. JHEP **03**, 076 (2010)
9. R. Dermisek, Unification of gauge couplings in the standard model with extra vectorlike families. Phys. Rev. D **87**(5), 055008 (2013)
10. L.-F. Li, F. Wu, Coupling constant unification in extensions of standard model. Int. J. Mod. Phys. A **19**, 3217–3224 (2004)
11. R. Shrock, Variants of the standard model with electroweak-singlet quarks. Phys. Rev. D **78**, 076009 (2008)
12. I. Dorsner, P. Fileviez Perez, Unification without supersymmetry: neutrino mass, proton decay and light leptoquarks. Nucl. Phys. **B723**, 53–76 (2005)
13. J.L. Chkareuli, I.G. Gogoladze, A.B. Kobakhidze, Natural nonSUSY SU(N) GUTs. Phys. Lett. B **340**, 63–66 (1994)
14. R. Dermisek, Insensitive unification of gauge couplings. Phys. Lett. B **713**, 469–472 (2012)
15. I. Dorsner, S. Fajfer, I. Mustac, Light vector-like fermions in a minimal SU(5) setup. Phys. Rev. D **89**(11), 115004 (2014)
16. M.-L. Xiao, J.-H. Yu, Stabilizing electroweak vacuum in a vectorlike fermion model. Phys. Rev. D **90**(1), 014007 (2014). [Addendum: Phys. Rev. D **90**(1), 019901 (2014)]
17. F. del Aguila, J. de Blas, M. Perez-Victoria, Effects of new leptons in electroweak precision data. Phys. Rev. D **78**, 013010 (2008)
18. S.A.R. Ellis, R.M. Godbole, S. Gopalakrishna, J.D. Wells, Survey of vector-like fermion extensions of the standard model and their phenomenological implications. JHEP **09**, 130 (2014)
19. B. Bhattacherjee, P. Byakti, A. Kushwaha, S.K. Vempati, Unification with vector-like fermions and signals at LHC. JHEP **05**, 090 (2018)
20. C. Patrignani and P. D. Group, Review of particle physics. Chinese Phys. C **40**(10), 100001 (2016)
21. D.R.T. Jones, The two loop beta function for a G(1) x G(2) gauge theory. Phys. Rev. D **25**, 581 (1982)
22. H. Arason, D.J. Castano, B. Keszthelyi, S. Mikaelian, E.J. Piard, P. Ramond, B.D. Wright, Renormalization group study of the standard model and its extensions. 1. The standard model. Phys. Rev. D **46**, 3945–3965 (1992)
23. D. Buttazzo, G. Degrassi, P.P. Giardino, G.F. Giudice, F. Sala, A. Salvio, A. Strumia, Investigating the near-criticality of the Higgs boson. JHEP **12**, 089 (2013)

24. V. Takhistov, Review of nucleon decay searches at super-Kamiokande, in *51st Rencontres de Moriond on EW Interactions and Unified Theories La Thuile, Italy, March 12–19, 2016* (2016)
25. R. Slansky, Group theory for unified model building. Phys. Rep. **79**, 1–128 (1981)
26. Y. Kats, M.J. Strassler, Probing colored particles with photons, leptons, and jets. JHEP **11**, 097 (2012). [Erratum: JHEP 07,009 (2016)]
27. Y. Kats, M.D. Schwartz, Annihilation decays of bound states at the LHC. JHEP **04**, 016 (2010)
28. G. Aad et al., Search for new phenomena in the dijet mass distribution using $p - p$ collision data at $\sqrt{s} = 8$ TeV with the ATLAS detector. Phys. Rev. D **91**(5), 052007 (2015)
29. V. Khachatryan et al., Search for narrow resonances in dijet final states at sqrt(s) = 8 TeV with the novel CMS technique of data scouting. Phys. Rev. Lett. **117**, 031802 (2016)
30. Search for New Phenomena in Dijet Events with the ATLAS Detector at $\sqrt{s}$ = 13 TeV with 2015 and 2016 data, Technical report. ATLAS-CONF-2016-069, CERN, Geneva (2016)
31. A.M. Sirunyan et al., Search for dijet resonances in proton-proton collisions at $\sqrt{s} = 13$ TeV and constraints on dark matter and other models (Phys. Lett. B, Submitted to, 2016)
32. Search for scalar diphoton resonances with 15.4 fb^{-1} of data collected at $\sqrt{s}$ = 13 TeV in 2015 and 2016 with the ATLAS detector, Technical report. ATLAS-CONF-2016-059, CERN, Geneva (2016)
33. V. Khachatryan et al., Search for high-mass diphoton resonances in proton-proton collisions at 13 TeV and combination with 8 TeV search (Phys. Lett. B, Submitted to, 2016)
34. K. Kowalska, D. Kumar, Road map through the desert: unification with vector-like fermions. JHEP **12**, 094 (2019)